ADVANCED FUNCTIONAL MATERIALS
www.afm-journal.de

Tethered Lipid Bilayer Gates: Toward Extended Retention of Hydrophilic Cargo in Porous Nanocarriers

*Jixi Zhang, Diti Desai, and Jessica M. Rosenholm**

A high-performance molecular gating system for efficient capping and delivery of hydrophilic cargo is reported. It integrates a mesoporous silica nanoparticle core and a lipid bilayer (LB) shell by covalent tethering via a hyperbranched polyethylenimine (PEI) cushion. When using calcein as a general model for hydrophilic drug molecules, a high payload is loaded into the porous structure due to greatly enhanced concentration of amino groups on the pore walls. Surprisingly, LB non-disruptively resides on the porous surface in this system, despite the strong positive charge from PEI, originating from the covalent tethering of the inner leaflet, as well as preferential spanning over the pore openings facilitated by the stretching of PEI chains on the particle surface. An unprecedented high retention of negatively charged hydrophilic guest molecules after up to 1 week is consequently achieved, even in the presence of a membrane disrupting agent. Furthermore, a PEI-induced charge conversion at neutral pH is conferred to the particles using a zwitterionic PC lipid as the outer leaflet of LB. Interestingly, the corresponding nanocarriers are able to promote cargo escape from endosomes. Subsequent delivery of the loaded hydrophilic cargo to the cytoplasm is observed despite the tight retention under extracellular conditions.

1. Introduction

Biomolecule-gated mesoporous silica nanoparticles (MSNs) have been receiving rapidly expanding attention as potential carriers for controlled drug delivery.[1] MSN supported lipid bilayers (LB), the so-called "protocell" structure, was recently pioneered by the induced liposome fusion[2] or self-assembly method.[3] The sophisticated architecture of such structures mimics the cell membrane's property on the impermeability towards hydrophilic molecules by the hydrophobic bilayer interior. Here, MSNs can carry high payloads of guest molecules owing to their high surface area and large accessible pore volumes, as well as impart LB with higher stability by solid supporting, while LB elegantly functions as a biomimetic cap facilitating barrier formation towards hydrophilic drugs loaded in MSNs. These advantages provide promising potential for the unique retention of hydrophilic drugs, a large fraction of which are in fact weak acids and thus negatively charged at physiological pH. The success of this approach hinge upon a high surface coverage of LB without losing the integrity that is needed for guest retention. However, limitations for generalizing such a design can be encountered when trying to use porous particles with varying surface properties including topography, local curvature, charging behavior etc., due to the physical proximity of LB to the underlying solid surface.[4] For instance, cationic particle surfaces, which is crucial for achieving a high payload of negatively charged guest molecules, can interact electrostatically with the residing LB and generally lead to the disruption or defects in the supported LB.[5] Furthermore, a consequent detachment or replacement by other surface-active components may take place in physiological fluids, thus leaving it susceptible to destabilization and rendering the membrane's lifetime too short for practical purposes.[6] This calls for a method which is capable of generating LB gated MSN with high loading capacity, prolonged retention of sequestered hydrophilic guests, and low premature leakage of cargo before cellular internalization.

A potential solution to minimize the influence from the particle surface is to introduce a soft layer to lift LB off the rough solid surface. Polymer cushioned bilayers is an excellent example of meta-materials that has features strikingly similar to the exquisite actin-membrane structure of living cells and may thus meet the abovementioned challenge.[7] In one promising approach for planar substrates, polymer tethers were also used to covalently attach the inner (proximal) lipid layer of LB to form a tethered LB (tLB) which can recapitulate basic properties of biological membranes to a further step.[8] Nevertheless, the translation of the tLB's advantages from planar substrate surface to the field of nanomedicine hasn't been explored yet, and presents a challenge of special significance.

According to our previous findings, hyperbranched polyethylenimine (PEI) functionalized on MSN surfaces can act as a molecular barrier to retain hydrophobic molecules loaded inside mesopores.[9] Herein, we report on the construction strategy of tLB on MSN surfaces mediated by hyperbranched PEI, as depicted in **Scheme 1**, with a focus on whether polymer tethering can be exploited to address the challenge of defect-free

Dr. J. Zhang, D. Desai, Dr. J. M. Rosenholm
Centre for Functional Materials
Laboratory for Physical Chemistry
Department of Natural Sciences
Åbo Akademi University
Porthansgatan 3–5, Turku, 20500, Finland
E-mail: jerosenh@abo.fi

DOI: 10.1002/adfm.201302995

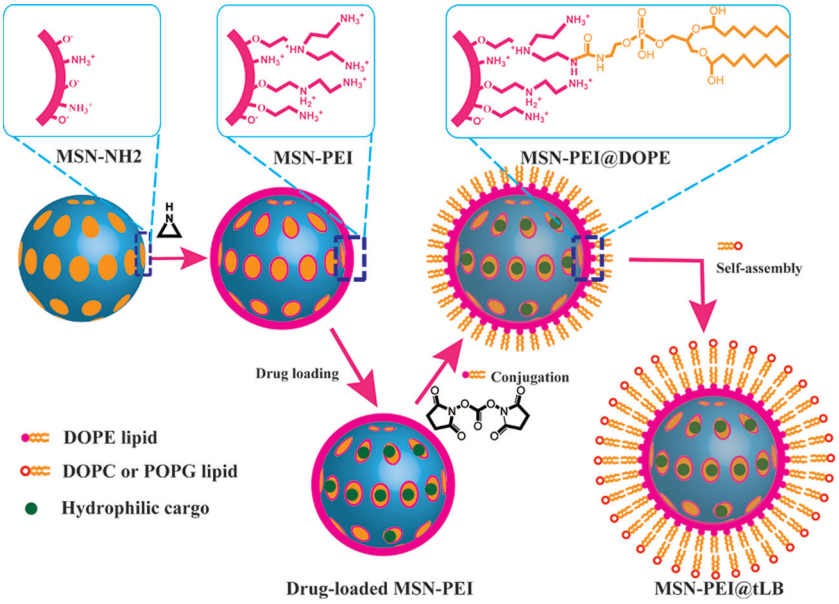

Scheme 1. Scheme demonstrating the LB tethering approach on MSN surface by hyperbranched PEI. Hyperbranched PEI (pink) was anchored onto the surface of amino group co-condensed MSN (MSN-NH_2) for the subsequent loading of negatively-charged drug (green dots). Thereafter, the conjugation of DOPE lipid as an inner leaflet of LB was realized by using a coupling agent *N,N'*-disuccinimidyl carbonate (DSC). The self-assembly of the outer leaflet of LB driven by hydrophobic interactions was carried out through a dual solvent exchange method in the final step.

and durable LB on solid nanocarriers. In the first step, hyperbranching surface polymerization of aziridine onto the surface of amino-functionalized MSN particles from a co-condensation approach (MSN-NH_2) was achieved according to our published procedures.[10] PEI plays an essential role to increase the amount of accessible amine groups, on the one hand for efficient cargo loading by electrostatic adsorption to the pore surfaces, and on the other hand for LB tethering on the particle's exterior surface. Next, the inner leaflet of LB composed by DOPE lipids was tethered via the covalent conjugation between primary amines of 1,2-dioleoyl-sn-glycero-3-phosphoethanolamine (DOPE) and that of PEI.[11] The densely packed hydrophobic tails of DOPE stretching outwards therefore led to the self-assembly of another phospholipid (zwitterionic DOPC or anionic POPG) driven by van der Waals interactions in a dual solvent exchange method, [12] resulting in the formation of the outer leaflet of tLB. PC and PG lipids, accounting for a large portion of the phospholipids in most mammalian cells, were employed in our materials since they are also common constituents of the popularly applied liposomes in nanomedicine. As a proof-of-concept for this strategy, the LB permeability and stability were subsequently studied by monitoring the retention of a loaded hydrophilic probe, calcein, in the internal MSN-PEI compartment. Subsequently, flow cytometry and cell fluorescence microscopy studies were carried out to evaluate the intracellular drug delivery ability of this LB gated MSN carrier.

2. Results and Discussion

2.1. Structural Characterization of the Hybrid Nanocarrier

As revealed by scanning electron microscopy (SEM, **Figure 1**A) and transmission electron microscopy (TEM, Figure 1B) images, uniform spherical MSN-NH_2 particles were synthesized with an average diameter of 70 nm as the starting material. Amino groups were modified on the particle surface by a co-condensation approach to facilitate an efficient surface polymerization of PEI.[10] TEM image of MSN-PEI particles stained with osmium (Figure 1C) clearly reveals the reduction in the contrast of the mesopores by the presence of a large amount of scattered black dots. Regarding the easy complexation between amines and osmium,[13] these dots can be ascribed to the hyperbranched polymers on both the exterior particle surface and interior mesopore surface. It should be mentioned that the thickness of the PEI modification layer on the pore surface is thinner than that on the

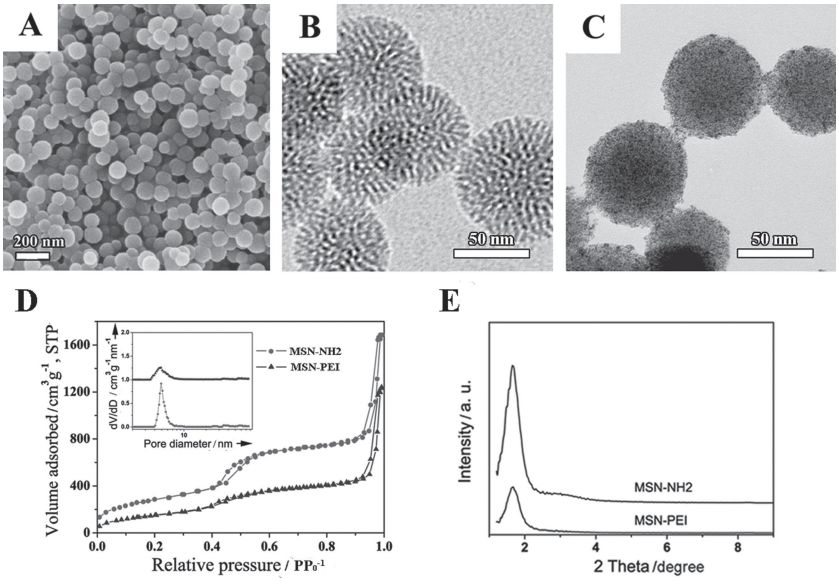

Figure 1. Representative SEM image of the starting particles (MSN-NH_2, A), TEM images of MSN-NH_2 (B) and the hyperbranched PEI modified MSNs (MSN-PEI, C). MSN-PEI sample was stained with osmium tetraoxide to show the presence of PEI. Typical nitrogen sorption isotherms (D), the corresponding pore size distributions (inset), and small angle X-ray diffraction patterns of MSN-NH_2 and MSN-PEI.

exterior particle surface, as also represented in Scheme 1. This effect was investigated and well discussed in our previous report.[10] The mechanism behind this is that the growth accompanying the branching in solution on flat surfaces usually stops after 3 or 4 generations (theoretically around 1.8 nm in thickness) due to steric encumbrance,[14] and the spatially restricted mesopore environment involves even more pronounced restrictions for a similar surface density of amines by the hyperbranching polymerization method in solvent.

The typical nitrogen adsorption-desorption isotherms for MSN-NH_2 and MSN-PEI confirmed the porous nature of the particles (Figure 1D). Compared with MSN-NH_2, the isotherm of MSN-PEI displays an apparently decreased specific surface area (from 1043 m^2 g^{-1} to 566 m^2 g^{-1}) and pore volume (from 0.85 cm^3 g^{-1} to 0.58 cm^3 g^{-1}), implying a successful polymer modification. The mesopore diameters decreased slightly after PEI polymerization although the peak position in the pore size distribution remained virtually unchanged (4.8 nm, Figure 1C inset). There were a significant reduction in the intensity of X-ray diffraction peak (Figure 1E) and a substantial increase in the weight loss (23 wt%) of the TGA curve (**Figure 2**B) for MSN-PEI, which further supports the successful surface polymerization.

Hyperbranching surface polymerization is a very promising method for amino functionalization of mesoporous silica, as the surface concentration of amine groups on MSN carriers can be much higher than what is normally achieved by silanization.[10] In this study, the total amounts of accessible primary amines on MSN-NH_2 and MSN-PEI were 0.471 mmol g^{-1} and 1.467 mmol g^{-1}, respectively, as determined by a nihydrin test (see Supporting Information). This threefold increase in the surface density of the accessible primary amines is a consequence of efficient hyperbranching surface polymerization. The primary amines on the particle's exterior surface are the terminal groups of the hyperbranched PEI structure, and they played an essential role in the tethering of NHS group activated DOPE lipids, as evidenced by the amide vibration peaks in the FTIR spectrum (Figure 2A) and a weight-loss increase of 8.4 wt% in the corresponding TGA curve (Figure 2B). Considering the calculations of the theoretical packing density of lipids in a single leaflet of LB (23500 per particle, see Supporting Information), the weight loss in TGA is close to that of ideal MSN@tLB particles in an ideally tight packing manner (11.5 wt%). This confirms that a well packed inner leaflet of LB composed by DOPE lipids was successfully tethered on the PEI layer. Moreover, the hyperbranched PEI molecules on the outlet pore perimeter would stretch away to the pore openings and facilitate the conjugation of DOPE over the pores by their terminal primary amines. The conjugation step thus left hydrophobic tails of DOPE pointing outwards.

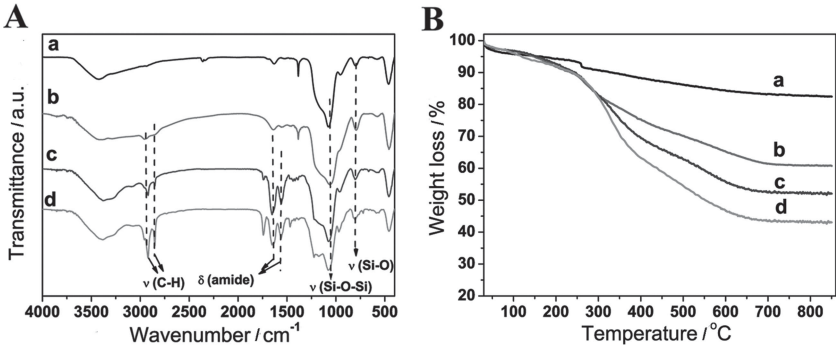

Figure 2. FTIR spectra (A) and TGA curves (B) of MSN-NH_2 (a), MSN-PEI (b), MSN-PEI@DOPE (c), and MSN-PEI@tLB (d). The peaks at 1650 cm^{-1} and 1560 cm^{-1} in FTIR spectrum for DOPE conjugated MSN-PEI can be ascribed to the vibrations of amide I and amide II from the conjugation between the primary amines of PEI and DOPE by DSC. The greatly enhanced bands at 2927 cm^{-1} and 2854 cm^{-1} correspond to the asymmetric and symmetric methylene stretching modes, respectively, from the alkyl tails of DOPE and DOPC.

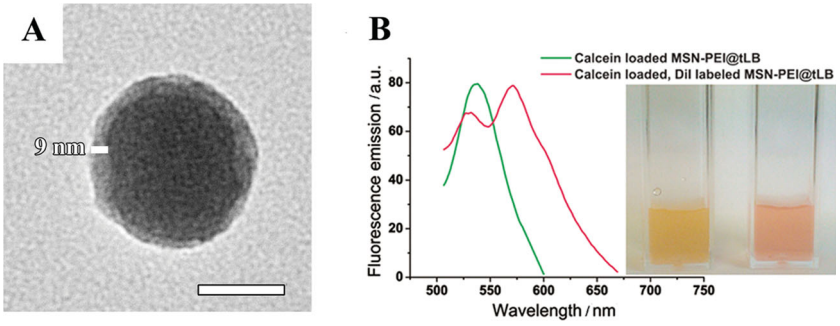

Figure 3. (A) Representative TEM images of the LB tethered nanocomposites (MSN@tLB). The sample was stained with osmium tetraoxide to show the presence of LB. Scale bar represents 50 nm. (B) Fluorescence emission spectra of calcein loaded MSN-PEI@tLB in water before and after the staining of the tLB's outer leaflet with a lipophilic dye DiI (inset shows the picture of the corresponding suspensions).

To confirm that the self-assembly of the outer leaflet of LB can be induced favorably by the tethered inner leaflet, we first performed osmium-stained TEM[15] for the as-obtained MSN-PEI@tLB particles with DOPC lipid as the outer leaflet. As shown in **Figure 3**A and Figure S1, individually encapsulated particles with typical core-shell morphology were obtained. The core region is darker than the shell, presumably because of the penetration of osmium into the pores of MSN-PEI particles. The thickness of the shell is around 9 nm, which should be contributed by a PEI tether layer and a lipid bilayer (typically 5–6 nm in thickness). Indeed, the average hydrodynamic diameter of MSN-PEI particles exhibited an increase of about 20 nm after the tethering of LB (**Figure 4**A). Furthermore, a weight-loss increase of 9.0 wt% in the TGA curve was found after the self-assembly step. This demonstrates that the outer leaflet of DOPC has the same molecular packing density as that of the inner leaflet of DOPE, further supporting the bilayer structure of tLB. Calcein loaded particles were then applied in the process to verify the coexistence of loaded calcein and the tethered LB in the composite particle by our strategy. After the

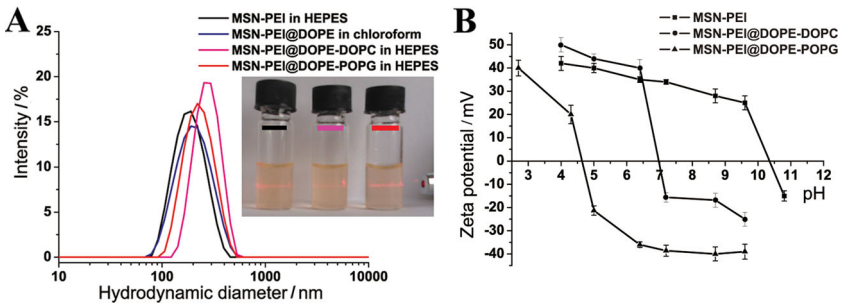

Figure 4. (A) Hydrodynamic diameter distributions of MSN-PEI, MSN-PEI@DOPE, and MSN-PEI@tLB with different composition. Inset shows a photograph of MSN-PEI, MSN-PEI@DOPE-DOPC, and MSN-PEI@DOPE-DOPC dispersed in HEPES buffer (pH 7.2). (B) Plots of zeta potential changing as a function of pH for MSN-PEI and MSN-PEI@LB with different composition of the outer leaflet.

outer leaflet of LB was stained by a lipophilic carbocyanine dye DiI which is weakly fluorescent until incorporated into the hydrophobic LB, a concomitant color change was clearly visible under light, as shown in Figure 3B. Interestingly, when excited at the same wavelength of 440 nm (for calcein) the emission spectrum of DiI stained particles showed a decrease in the peak fluorescence of calcein and an arising new peak of DiI (575 nm) compared to particles loaded with calcein only. This should be attributed to the fluorescence resonance energy transfer (FRET) from calcein to DiI (Figure S2) considering that the distance between the calcein molecules on the pore openings and the DiI molecules in LB is within the FRET interaction range. These results strongly support the reliability of our proposed strategy for the construction of tLB on MSN surfaces. In contrast, in a control experiment using MSN-NH_2 as the solid core, a very large increase in both the average diameter and the polydispersity index (PDI) were found in the hydrodynamic diameter distribution of particles following the same LB-tethering process (Figure S3), indicative of a strong aggregation possibly resulting from defect-containing noncontinuous LB.

To elucidate the generality of this method, we further tested the possibility of the self-assembly of POPG, an anionic charged lipid, on the DOPE tethered MSN-PEI particles. A narrow peak was also observed in the hydrodynamic diameter distribution of MSN-PEI@DOPE-DOPC, suggesting its monodispersity in aqueous solution. The peak position was slightly larger than that of MSN-PEI@DOPE-POPG. Zeta potential measurements were performed to compare the surface properties of MSN-PEI@tLB with different composition (Figure 4B). Given the charging behavior of PC and PG lipids,[16] it is surprising that the tethered LB coated on the particles did not notably impart them with similar surface charging properties as the phospholipids (pKa 1.0 for PC lipids, pKa 3 for PG lipids). Instead, the LB coating shifted the isoelectric point (IEP) of MSN-PEI particles from 10.4 to 7.0 and 4.6 for MSN-PEI@DOPE-DOPC and MSN-PEI@DOPE-POPG, respectively. Certainly, the underlying PEI affected the charging of the whole particle by its strong 'proton sponge' ability. However, the outer surface of MSN-PEI@tLB is constituted by lipids with high packing density, which made the charging most closely associated with DOPC or POPG. The difference in the pH-dependent surface charging after LB tethering should be owing to the long-range influence of the underlying PEI layer on the outer lipids. The charge conversion from negative (-15 mV) to highly positive (+40 mV) at neutral pH for MSN-PEI@DOPE-DOPC would facilitate the escape of the particles and/or cargo from weakly acidic endolysosomal compartvments after cellular internalization.[9]

2.2. Loading and Retention of Hydrophilic Cargo

Based on the successful construction of tLB on pure MSNs, the hydrophilic guest calcein was then loaded prior to the conjugation of DOPE inner leaflet. As the conjugation reaction was carried out in organic solvents, there was no leakage of calcein in the tethering process due to its low solubility in these solvents. The use of hyperbranched polyethyleneimine (PEI), which is positively charged in aqueous solutions below pH 10, allows for electrostatic adsorption of the negatively charged hydrophilic guest molecules onto the polyelectrolyte-grafted substrate. The saturated loading degree of calcein for MSN-PEI was 42 wt% with respect to particle weight, obtained by adsorption from MES buffer (pH 5, **Figure 5**). The surface-area-normalized loading capacity of calcein on MSN-PEI (0.74 mg m^{-2}), was nearly 3 fold to that of MSN-NH_2 (0.27 mg m^{-2}) resulting from the greatly enhanced surface concentration of amino groups after the hyperbranching surface polymerization. To further understand the adsorption behavior of these materials, calcein adsorption capacities were normalized to the total amount of accessible primary amines, which gave calcein/primary amine molar ratios of 0.95 and 0.46 for MSN-NH_2 and MSN-PEI, respectively. The data demonstrates that the lower surface density of amino groups on MSN-NH_2 allowed for

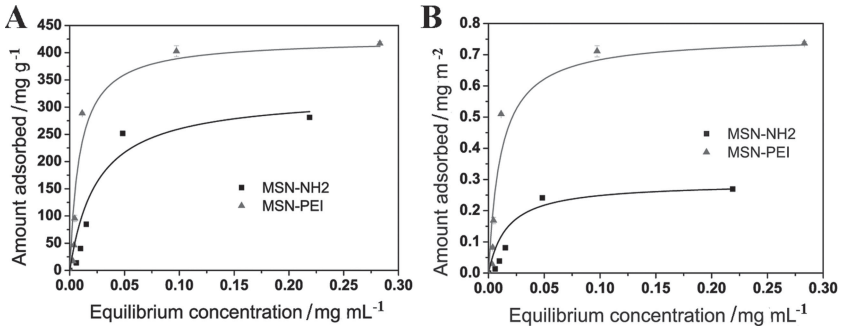

Figure 5. Typical adsorption isotherms (A) of calcein on MSN-NH_2 and MSN-PEI in MES buffer (pH 5) solution. The loading capacity is around 280 mg g^{-1} and 420 mg g^{-1} for MSN-NH2 and MSN-PEI, respectively. These values can be converted to 0.27 mg m^{-2} for MSN-NH2 and 0.74 mg m^{-2} for MSN-PEI when normalized against surface areas (B).

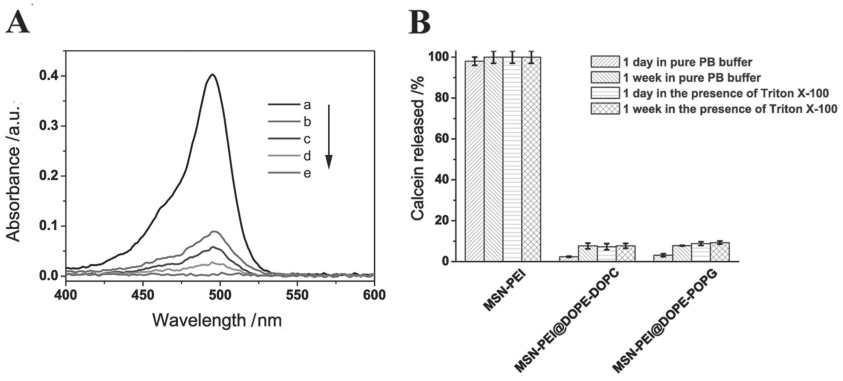

Figure 6. (A) Absorption spectra of the release supernatant from calcein loaded MSN-PEI (a), and MSN-PEI@tLB particles prepared by using different volume fractions of water in the phase transfer step of the LB self-assembly process: 0 vol% (b), 80 vol% (c), 90 vol% (d), 95 vol% (e). Calcein was loaded into MSNs at a loading degree of 90 μg mg^{-1} and the particles were incubated in 20 mM PB buffer (pH 7.4) at a concentration of 0.5 mg mL^{-1}. (B) Long term calcein release evaluated by the absorbance at 497 nm for the supernatant from different calcein loaded particles in PB buffer with or without Triton X-100 (a membrane disrupting agent) after different time periods.

an almost complete occupation of positively charged binding sites, as expected for an electrostatic adsorption. By contrast, high amino density in the case of MSN-PEI resulted in much more steric hindrance for the accommodation of calcein molecules onto the PEI layer. Meanwhile, we should also take into account that the stretching of the hyperbranched structure inside the mesopores would also cause additional diffusion and space limitations for every amine to take part in the adsorption.

The most important advantage of LB results from their ability to retain hydrophilic guest molecules. This was clearly illustrated in **Figure 6**A, where in the absence of tLB gating, calcein loaded in MSN-PEI was quickly replaced by anions in the release media, resulting in a complete premature release. Of particular importance for this tLB strategy also involves the generation of a closely packed outer leaflet of LB with extended durability. In our approach, a dual solvent exchange method, by changing solvent system from chloroform to DMSO to water, was employed to generate a gradual increase of the solvent polarity for inducing the self-assembly.[12] To maximize the retention efficiency of drug, we then optimized the volume ratio of water/DMSO to testify the influence of solvent polarity on the sealing efficiency of LB. The premature release was reduced dramatically by 77–100% compared with that of MSN-PEI when increasing the DMSO volume. Zero release was achieved by utilizing 95 vol% water in the self-assembly process, indicative of an intact LB and in turn a high enough sequestering of hydrophilic guests at this polarity. Moreover, long term evaluation indicated that there was still a quite low release (less than 10%) after one week of incubation in PB buffer (Figure 6B). Additionally, the presence of a membrane-disrupting agent, Triton X-100,[3a] in the release medium did not lead to a conventionally rapid and continuous release of the loaded cargo. Instead, a low absorbance of calcein in the supernatant, comparable to that in the absence of Triton X-100, was observed and remained with time up to 1 week, suggesting a greatly enhanced durability of the tethered LB. The same retention efficiency was also observed in the system of MSN-PEI@DOPE-POPG (Figure 6B).

The above results are apparently not in accordance with the previous study on LB systems physically supported on a cationic surface, where defects were induced.[2b] The intermediate PEI succeeded in non-disruptively lifting off LB from the porous particle surface. Interactions of cationic polymers with lipid bilayers and live cell membranes have been extensively investigated in the past decade.[17] It was reported that polymers like PEI, possessing high density of positively-charged groups, can induce two basic types of disruption, membrane hole formation and membrane thinning via the reorientation of lipids or the removal of a layer of lipid from the lipid bilayers.[5,18] However, these two kinds of LB disruption require a close spatial proximity (<1 nm) between the headgroups of phospholipids and polymer, so that local short-range interactions can take place to generate the reorientation/reorganization of lipids.[19] In the case of tLB, the local interaction between PEI and the inner leaflet of LB was substituted by covalent conjugation. Meanwhile, the thickness of LB separated the outer leaflet of LB from direct interaction with the charged amine groups of PEI. More importantly, the Coulombic repulsion between amino groups would make the PEI chains in the external surface adopt a rigidlike conformation and be pushed away toward the pore openings, as previously observed in mesoporous silica particles functionalized with polyamines.[20] This would also be beneficial for PEI tethered LB to span over the pore openings in the self-assembly process, as supported by the aforementioned result in the control experiment where the aminopropyl groups on MSN-NH_2 particles did not form a continuous LB. The combination of these factors may lead tLB in our strategy to prefer packing more defect-free and durable.

2.3. Intracellular Delivery

The potential of MSN-PEI@tLB system to deliver hydrophilic guests to cells was analyzed by the degree of cellular internalization of calcein. First, the cell viability in the presence of the carriers was confirmed, and both MSN-PEI@tLB particles exhibited HeLa cell viability higher than 90% at the investigated particle concentrations (Figure S4A). In the intracellular delivery ability evaluation, an increase of MSN-PEI particles' concentration from 10 μg mL^{-1} to 25 μg mL^{-1} did not lead to a significant enhancement of the mean fluorescence steaming from intracellular calcein in the cells (Figure S4B). However, a significant particle-dose-dependent increase in the mean fluorescence intensity was found for MSN-PEI@tLB particles. Particles loaded with calcein were incubated with HeLa cells at 10 μg mL^{-1} for up to 24 h and the fluorescence of calcein was recorded in the green channel on both a flow cytometer and a confocal fluorescence microscope. Very low calcein uptake was observed for MSN-PEI, as evident from slightly increased

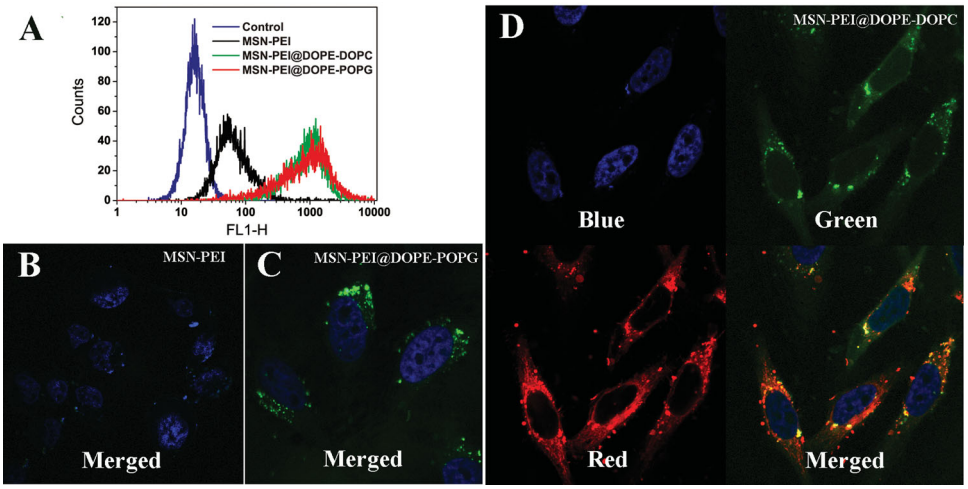

Figure 7. (A) Flow cytometry histogram of HeLa cells after incubating with 10 μg mL^{-1} of MSN-PEI or MSN-PEI@tLB (loaded with 9 wt% of calcein for 24 h. Higher intensity along the x axis (FL1-H) indicates more calcein delivered into the cells by the particles. (B–D) Corresponding confocal fluorescence microscopy images of HeLa cells incubated with calcein-loaded MSN-PEI (B), MSN-PEI@DOPE-POPG (C), MSN-PEI@DOPE-DOPC (D). Green and red channel shows the presence of calcein and DiI, respectively. Blue channel shows cell nuclei stained by 4',6-dia-midino-2-phenylindole (DAPI).

fluorescence intensity in the fluorescence histogram of cells (**Figure 7**A) and negligible green signal in the fluorescence microscope image (Figure 7B). This result is in line with the results from Figure 3A where calcein displacement by anions was observed, whereby most calcein would be released already outside the cells prior to cellular uptake of the particles. Consequently, there would be only negligible delivery regarding that calcein is a typical cell-membrane impermeable fluorescent probe.[21]

In contrast, LB tethered particles produced a significantly strong fluorescence signal inside the cells (Figure 7C,D), implying improved calcein retention before and during the cellular internalization of the carrier particles. Furthermore, a localized dotted pattern of green coloration around the nuclei was also observed in both MSN-PEI@tLB systems (DOPC or POPG as the outer leaflet of LB), indicating typical endocytosis of nanoparticles followed by compartmentalizing inside endosomes or lysosomes. In comparison with MSN-PEI@DOPE-POPG, there were more green signals spreading through the cells in the case of MSN-PEI@DOPE-DOPC. This difference was much more significant after 48 h of incubation (**Figure 8**). Regarding the surface charge conversion of MSN-PEI@DOPE-DOPC particles to a highly positive value in acidic environment, it is possible that utilizing of DOPC as the outer leaflet of LB could make the guest molecules escape from endosomes easier and thus be delivered to the cytoplasm more efficiently.[9,22] In order to also track the intracellular location of the LB, DiI staining of the outer leaflet was used in the fluorescence microscopy study. As shown in the red channel of Figure 8D, DiI was distributed throughout the whole cell. Although the tethered LB can be tightly retained in the extracellular condition, exchange and redistribution of lipids within the intracellular membranes and other intracellular components could still lead to the disassembly of the outer leaflet which, in turn, promotes release of the entrapped cargo.

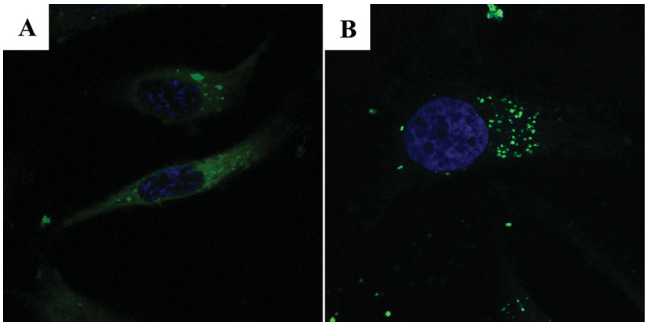

Figure 8. Confocal fluorescence microscopy images of HeLa cells after incubation with 10 μg mL^{-1} of calcein-loaded MSN-PEI@DOPE-DOPC (A) and MSN-PEI@DOPE-POPG (B) for 48 h, indicating clear difference in the intracellular delivery pattern of calcein loaded in these two different particles.

3. Conclusion

We have demonstrated the first example that hyperbranched PEI modified on MSN surfaces could serve as a robust and efficient cushion for the tethering of lipid bilayers by conjugation and self-assembly methods, leading to the formation of a novel hybrid material. Our results have shown that PEI modified on pore surfaces facilitates a high loading of negatively-charged hydrophilic guest molecules, while those on the particle's external surface induced a densely packed defect-free and durable LB for sealing cargo within the mesopores. Thus, the cargo retention remained after up to 1 week even in the presence of a membrane disrupting agent. Moreover, the surface charging of the LB coated composite particles was greatly altered by PEI, making their possible application consequently more attractive. In particular, employing the zwitterionic lipid DOPC as the outer leaflet of LB, we were able to demonstrate that the resultant particles were imparted with a charge

conversion property at neutral pH and consequently able to aid the cargo escape from the endosomes into the cytoplasm, which is essential for successful intracellular delivery. As the result of molecular engineering inspired by biology, we anticipate that our findings may pave a facile and distinctive way to construct biomimetic LB on porous nanocarriers towards efficient retention and delivery of guest molecules.

4. Experimental Section

Materials: Unless otherwise noted, all reagent-grade chemicals were used as received, and Millipore water was used in the preparation of all aqueous solutions. Cetylmethylammonium bromide (CTAB, AR) was purchased from Fluka. 1, 3, 5-trimethyl-benzene (TMB, 99%) was purchased from ACROS. Decane (99%) was purchased from Alfa Aesar. Anhydrous toluene (AR), anhydrous chloroform (AR), anhydrous DMF (AR), ethylene glycol (AR), tetraethyl orthosilicate (TEOS, AR), 3-aminopropyltriethoxysilane (APTES, AR), NH_4OH (30 wt.%, AR), *N,N′*-disuccinimidyl carbonate (DSC), *N,N′*-dimethylaminopyridine (DMAP), 1,2-dioleoyl-sn-glycero-3-phosphoethanolamine (DOPE, lyophilized powder), 1,2-dioleoyl-sn-glycero-3-phosphocholine (DOPC, lyophilized powder), (2Z)-2-[(E)-3-(3,3-dimethyl-1-octadecylindol-1-ium-2-yl)prop-2-enylidene]-3,3-dimethyl-1-octadecylindole perchlorate (DiI, lyophilized powder) were purchased from Sigma. 1-palmitoyl-2-oleoyl-sn-glycero-3-phospho-(1'-rac-glycerol) (POPG, sodium salt) was purchased from Genzyme. Aziridine was synthesized from aminoethylsulfuric acid (Aldrich) according to the procedure described by Allen et al.[23]

Synthesis of Amino Group Modified MSNs (MSN-NH_2): The starting particles were prepared by co-condensation procedure using TEOS and APTES as silica source according to the recipe reported by us.[24] In a typical experimental procedure, firstly a mixed solution was prepared by dissolving and heating CTAB (0.45 g) in a mixture water (150 mL) and ethylene glycol (30 mL) at 70 °C in a flask reactor. After a clear solution was obtained, decane (2.1 mL) was subsequently added to the system. Then, 1,3,5-trimethylbenzene (TMB, 0.51 mL) was added into the mixture after 0.5 h and stirring continued for another 1.5 h to homogenize the solution. Ammonium hydroxide (30 wt%, 2.5 mL) was introduced to the system as catalyst before TEOS (1.5 mL) and APTES (0.3 mL) was added consecutively to initiate the reaction. The molar ratio used in the synthesis was 1 TEOS: 0.19 APTES: 0.18 CTAB: 0.55 TMB: 1.6 decane: 5.9 NH_3: 88.5 ethylene glycol: 1249 H_2O.The reaction was allowed to proceed for 3 h at 70 °C. Then, the heating was stopped and the as-synthesized colloidal suspension was then aged at 70 °C without stirring for 24 h. After the suspension was cooled to room temperature, the suspension was separated by centrifugation (at a rate of 9000 rpm). Ethanol was used to wash the centrifuged particle. The template removal was performed by a highly efficient ion-exchange method. The purified nanoparticles were redispersed in a solution containing 60 mg ammonium nitrate in 20 mL of ethanol, and then the mixture was stirred at 60 °C for 30 min. The procedure was repeated three times to completely remove the surfactants. The final product was suspended in acetone for further use.

Synthesis of Hyperbranched PEI Modified MSNs (MSN-PEI): MSN-PEI particles were synthesized according to the previous paper by us.[10] Functionalization by surface grown poly (ethylene imine) (PEI) was obtained by acid-catalyzed hyperbranching surface polymerization of aziridine to increase the surface concentration of amino groups on the mesopore walls. A typical synthesis was performed with toluene as solvent. MSN-NH_2 particles from the previous synthesis step were centrifuged, washed with toluene two times. Then the toluene suspension (20 mL) was subsequently subjected to argon atmosphere. Catalytic amounts of acetic acid were added under stirring, after which aziridine was added in an amount of 0.5 mL per gram of particles. The suspension was stirred under argon atmosphere overnight at 70 °C, centrifuged, washed with toluene, and dispersed in acetone finally.

Calcein Loading into MSN-PEI: Calcein loading into MSN-PEI was performed by soaking particles in a solution of calcein in MES buffer (pH 5.0). For calcein adsorption isotherm measurements, MSN-PEI (2 mg) was suspended in water (2 mL) with different initial concentrations of calcein (0.1–0.7 mg mL^{-1}). Subsequently, the mixture was homogenized by continuous vibration at 25 °C for 8 h. The calcein-loaded MSN-PEI particles were separated by centrifugation and the supernatant liquid was collected. The amount of calcein adsorbed by MSN-PEI was calculated through the UV absorbance difference in the supernatant before and after the adsorption at a wavelength of 497 nm using a UV-Vis Spectrophotometer (NanoDrop 2000c, Thermo).

Surface Conjugation of DOPE Lipid to MSN-PEI: The inner leaflet of the lipid bilayer, DOPE, was covalently linked to MSN-PEI (with loaded drug or not) by a typical conjugation method using *N,N′*-disuccinimidyl carbonate (DSC) as a coupling agent,[11,25] where the primary amines of DOPE and PEI was crosslinked by an urea bond. First, the amine group of DOPE was reacted with DSC to obtain a NHS group terminated, amine reactive derivative, as shown in Scheme S1. Typically, DOPE solution in chloroform (0.3 mL, 4 mg mL^{-1}) was mixed with DSC solution in anhydrous DMF (0.128 mL, 4 mg mL^{-1}). Then *N,N′*-dimethylaminopyridine (DMAP, 4 mg mL^{-1} in anhydrous DMF, 0.12 mL) was subsequently introduced to the mixture in the presence of activated molecular sieves (3 Å). The molar ratio used in this NHS activation reaction was 1.6 DOPE: 2 DSC: 2 DMAP. The reaction was allowed to proceed for 7 h at room temperature under argon atmosphere. Second, MSN-PEI particles were directly introduced to the NHS modified DOPE lipid solution to accomplish the crosslinking. The coupling reaction was carried out at room temperature overnight. After that, the product particles were separated by centrifugation and washed with chloroform two times. Due to the low polarity of the organic solvents, there was no release of the hydrophilic probe, i.e. calcein, out from MSN-PEI during the crosslinking reaction.

Fabrication of Lipid Bilayers (LB) Coated MSNs (MSN-PEI@tLB): We used a novel dual solvent exchange method reported by Bao and co-workers,[12] in which solvent transition from chloroform to a more polar DMSO and then to water, facilitated the self-assembly of the outer leaflet of LB on MSN-PEI@DOPE. Compared with traditional film hydration method for lipid membranes, this strategy was demonstrated to be more efficient, require less purification, prevent aggregation, and overcome the heterogeneity of samples during the preparation. In a typical process, the MSN-PEI@DOPE particles from the above step were suspended in 0.1 mL chloroform solution of the second lipid (the neutral one DOPC or the negatively charged one POPG as shown in Scheme S2, 3 mg mL^{-1}). Then DMSO (0.5 mL) was added slowly to the mixture. The mixture was incubated with shaking at room temperature for 30 min. Chloroform was removed completely by vaporization under vacuum at 30 °C. Subsequently, deionized water was added to the suspension in DMSO under sonication to reach a varying total volume between 2.5 and 10 mL (corresponding to 80–95 vol% of water in the mixed solvent). DOPC lipids were mixed with a small fraction (2 mol%) of a lipophilic dye DiI (Scheme S3) at this step to stain the outer leaflet of LB. DMSO was substituted with water by three rounds of centrifugation at 8000 rpm for 15 min. The MSN-PEI@tLB product was dispersed in water for further use.

Detection of Calcein Release: Calcein was loaded into MSNs at a loading degree of 90 μg mg^{-1} and the loaded particles were incubated at 37 °C in 20 mM PB buffer (pH 7.4) at a concentration of 0.5 mg mL^{-1}. Particles were separated by centrifugation at different time periods. The amount of calcein released into the solution was analyzed through the UV absorbance in the supernatant at a wavelength of 497 nm using a UV-Vis Spectrophotometer (NanoDrop 2000c, Thermo). The stability of LB capped MSN for the retention of calcein was also evaluated against the non-ionic surfactant Triton X-100, a membrane disrupting agent. All experimental conditions were kept the same except the addition of Triton X-100 (10 μL) in the release medium (2 mL).

Cell Culturing and In vitro Experiments: HeLa (Human cervical carcinoma) cells obtained from ATCC (Manassas, VA, USA) were maintained in DMEM medium (Sigma, St. Louis, MO, USA)

supplemented with 10% fetal calf serum (Boiler, Wiltshire, UK), 2 mM L-glutamine, 100 U mL^{-1} penicillin, 100 µg mL^{-1} streptomycin at 37 °C in a 5% CO_2/95% O_2 and 90% RH humidify atmosphere.

Cell Viability Assay: HeLa cells were transferred to 96-well plates (9000 cells per well) and allowed to attach and grow up to ~70% confluence. After incubation, the old media was removed, cells were washed and new media containing MSN-PEI particles and MSN-PEI@tLB particles with different composition (10 and 25 µg mL^{-1}) in serum free DMEM media were added. After incubation for 24 h, WST-1 reagent (10 µL, Roche Applied Science, Upper Bavaria, Germany) was added to the cells and further incubated for 90 min; after which, the 96-well plate was analyzed at a 430 nm wavelength in a Varioskan plate reader (Thermo Scientific, Logan UT, USA) to determine cell viability. Here, the control group was the cell media only in the absence of particles.

Cellular Uptake Studies by FACS: To study cellular uptake, 10 and 25 µL of MSN-PEI particle suspensions (1 mg/mL) and MSN-PEI@tLB particles with different composition were mixed with 1 mL of serum free DMEM media. HeLa cells (9.0×10^4 cells per well) were cultured in a 12-well plate and grown to ~70% confluence. The old media was removed, cells were washed and new media containing MSN-PEI particles and MSN-PEI@tLB particles with different composition were added and incubated for 12 h at 37 °C. After the incubation cells were washed twice with PBS, treated with 400 µL of trypsin/EDTA solution (0.25% trypsin, 0.53 mM EDTA) at 37 °C for 5 min. The detached cells were then centrifuged and transferred to 500 µL PBS for flow cytometry studies. The amount of endocytosed particles was analyzed by BD FacsCalibur flow cytometer (FL-1, BD Pharmingen). The mean fluorescence intensity (MFI) of the cells at FL-1 channel was measured. The data was analyzed with BD CellQuest Pro software for total amount of MSNs uptaken by 10 000 cells. The bar graphs in the figures represent mean values (±SD) from four or more independent experiments.

Cellular Uptake Studies by Confocal Microscopy: HeLa cells (4.0×10^4 cells per well) were seeded on 24-well plate one day before treatment and incubated with 10 µg/mL MSN-PEI particles and MSN-PEI@tLB particles in serum free DMEM media for 24 h and 48 h. After incubation cell media was removed and cells were washed with PBS, and fixed with 4% paraformaldehyde (PFA), the nucleus was stained using VECTASHIELD Mounting Medium with DAPI (Vector Laboratories, Inc., Burlingame, USA). The localization of particles was viewed and imaged with Zeiss LSM510 Meta confocal microscope (100× oil immersion objective, 405 nm/488 nm/543 nm excitation) using Zen 2010 software and confocal images with blue (for DAPI), green (for calcein) and/or red (for DiI) channels were acquired.

Supporting Information

Supporting Information is available from the Wiley Online Library or from the author.

Acknowledgements

The financial support by the Magnus Ehrnrooth Foundation (J.Z.), Centre for International Mobility (CIMO) of Finland (D.D.) and The Academy of Finland projects #137101, 140193 and 260599 are greatly acknowledged. We would also like to acknowledge the assistance by Markus Peurla and Björn Enberg from University of Turku during the TEM characterization.

Received: August 27, 2013
Revised: October 15, 2013
Published online: December 16, 2013

[1] a) S. Wu, X. Huang, X. Du, *Angew. Chem. Int. Ed.* **2013**, *52*, 5580–5584; b) P. Yang, S. Gai, J. Lin, *Chem. Soc. Rev.* **2012**, *41*, 3679–3698; c) Z. Luo, K. Cai, Y. Hu, L. Zhao, P. Liu, L. Duan, W. Yang, *Angew. Chem. Int. Ed.* **2011**, *50*, 640–643; d) A. Agostini, L. Mondragón, A. Bernardos, R. Martínez-Máñez, M. D. Marcos, F. Sancenón, J. Soto, A. Costero, C. Manguan-García, R. Perona, *Angew. Chem. Int. Ed.* **2012**, *51*, 10556–10560.

[2] a) J. Liu, A. Stace-Naughton, X. Jiang, C. J. Brinker, *J. Am. Chem. Soc.* **2009**, *131*, 1354–1355; b) J. Liu, X. Jiang, C. Ashley, C. J. Brinker, *J. Am. Chem. Soc.* **2009**, *131*, 7567–7569; c) C. E. Ashley, E. C. Carnes, G. K. Phillips, D. Padilla, P. N. Durfee, P. A. Brown, T. N. Hanna, J. Liu, B. Phillips, M. B. Carter, N. J. Carroll, X. Jiang, D. R. Dunphy, C. L. Willman, D. N. Petsev, D. G. Evans, A. N. Parikh, B. Chackerian, W. Wharton, D. S. Peabody, C. J. Brinker, *Nat Mater.* **2011**, *10*, 389–397; d) E. Bringas, O. Koysuren, D. V. Quach, M. Mahmoudi, E. Aznar, J. D. Roehling, M. D. Marcos, R. Martinez-Manez, P. Stroeve, *Chem. Commun.* **2012**, *48*, 5647–5649.

[3] a) V. Cauda, H. Engelke, A. Sauer, D. Arcizet, C. Bräuchle, J. Rädler, T. Bein, *Nano Lett.* **2010**, *10*, 2484–2492; b) R. A. Roggers, V. S. Y. Lin, B. G. Trewyn, *Mol. Pharm.* **2012**, *9*, 2770–2777; c) L.-S. Wang, L.-C. Wu, S.-Y. Lu, L.-L. Chang, I. T. Teng, C.-M. Yang, J.-a. A. Ho, *ACS Nano* **2010**, *4*, 4371–4379.

[4] Y. Roiter, M. Ornatska, A. R. Rammohan, J. Balakrishnan, D. R. Heine, S. Minko, *Nano Lett.* **2008**, *8*, 941–944.

[5] P. R. Leroueil, S. A. Berry, K. Duthie, G. Han, V. M. Rotello, D. Q. McNerny, J. R. Baker, B. G. Orr, M. M. Banaszak Holl, *Nano Lett.* **2008**, *8*, 420–424.

[6] J. A. Zasadzinski, B. Wong, N. Forbes, G. Braun, G. Wu, *Curr. Opin. Colloid Interface Sci.* **2011**, *16*, 203–214.

[7] a) R. Naumann, S. M. Schiller, F. Giess, B. Grohe, K. B. Hartman, I. Kärcher, I. Köper, J. Lübben, K. Vasilev, W. Knoll, *Langmuir* **2003**, *19*, 5435–5443; b) J. Y. Wong, C. K. Park, M. Seitz, J. Israelachvili, *Biophys. J.* **1999**, *77*, 1458–1468; c) F. Roder, O. Birkholz, O. Beutel, D. Paterok, J. Piehler, *J. Am. Chem. Soc.* **2013**, *135*, 1189–1192.

[8] a) M. Tanaka, E. Sackmann, *Nature* **2005**, *437*, 656–663; b) C. A. Naumann, O. Prucker, T. Lehmann, J. Rühe, W. Knoll, C. W. Frank, *Biomacromolecules* **2001**, *3*, 27–35.

[9] a) J. M. Rosenholm, E. Peuhu, J. E. Eriksson, C. Sahlgren, M. Lindén, *Nano Lett.* **2009**, *9*, 3308–3311; b) V. Mamaeva, J. M. Rosenholm, L. T. Bate-Eya, L. Bergman, E. Peuhu, A. Duchanoy, L. E. Fortelius, S. Landor, D. M. Toivola, M. Linden, C. Sahlgren, *Mol. Ther.* **2011**, *19*, 1538.

[10] J. M. Rosenholm, M. Lindén, *Chem. Mater.* **2007**, *19*, 5023–5034.

[11] G. T. Hermanson, *Bioconjugate Techniques*, 2nd Ed., Elsevier, Rockford, USA, **2008**, pp.196–197.

[12] S. Tong, S. Hou, B. Ren, Z. Zheng, G. Bao, *Nano Lett.* **2011**, *11*, 3720–3726.

[13] R. Sanz, G. Calleja, A. Arencibia, E. S. Sanz-Pérez, *Microporous Mesoporous Mater.* **2012**, *158*, 309–317.

[14] D. A. Tomalia, A. M. Naylor, W. A. Goddard, *Angew. Chem. Int. Ed.* **1990**, *29*, 138.

[15] R. J. Collin, W. P. Griffith, *J. Histochem. Cytochem.* **1974**, *22*, 992–993.

[16] a) E. K. Perttu, A. G. Kohli, F. C. Szoka, *J. Am. Chem. Soc.* **2012**, *134*, 4485–4488; b) A. Dickey, R. Faller, *Biophys. J.* **2008**, *95*, 2636–2646.

[17] a) A. Mecke, I. J. Majoros, A. K. Patri, J. R. Baker, M. M. Banaszak Holl, B. G. Orr, *Langmuir* **2005**, *21*, 10348–10354; b) A. Mecke, D.-K. Lee, A. Ramamoorthy, B. G. Orr, M. M. Banaszak Holl, *Langmuir* **2005**, *21*, 8588–8590; c) C. L. Ting, Z.-G. Wang, *Biophys. J.* **2011**, *100*, 1288–1297.

[18] S. Hong, P. R. Leroueil, E. K. Janus, J. L. Peters, M.-M. Kober, M. T. Islam, B. G. Orr, J. R. Baker, M. M. Banaszak Holl, *Bioconjugate Chem.* **2006**, *17*, 728–734.

[19] a) L. Wang, M. Schönhoff, H. Möhwald, *J. Phys. Chem. B* **2002**, *106*, 9135–9142; b) A. Mecke, S. Uppuluri, T. M. Sassanella, D.-K. Lee, A. Ramamoorthy, J. R. Baker Jr, B. G. Orr, M. M. Banaszak Holl, *Chem. Phys. Lipids* **2004**, *132*, 3–14.

[20] a) R. Casasús, M. D. Marcos, R. Martínez-Máñez, J. V. Ros-Lis, J. Soto, L. A. Villaescusa, P. Amorós, D. Beltrán, C. Guillem, J. Latorre, *J. Am. Chem. Soc.* **2004**, *126*, 8612–8613; b) R. Casasús, E. Climent, M. D. Marcos, R. Martínez-Máñez, F. Sancenón, J. Soto, P. Amorós, J. Cano, E. Ruiz, *J. Am. Chem. Soc.* **2008**, *130*, 1903–1917.
[21] B. Maherani, E. Arab-Tehrany, A. Kheirolomoom, D. Geny, M. Linder, *Biochimie* **2013**, *95*, 2018.
[22] W. T. Godbey, K. K. Wu, A. G. Mikos, *J. Controlled Release* **1999**, *60*, 149.
[23] C. F. H. Allen, F. W. Spangler, E. R. Webster, *Organic Synthesis* (Ed: N. Rabjohn), Wiley, New York **1963**; p.433.
[24] J. Zhang, J. M. Rosenholm, H. Gu, *ChemPhysChem* **2012**, *13*, 2016–2019.
[25] B. Guan, A. Magenau, K. A. Kilian, S. Ciampi, K. Gaus, P. J. Reece, J. J. Gooding, *Faraday Discussions* **2011**, *149*, 301–317.